INSTITUTE OF PHYSICS PUBLISHING JOURNAL OF OPTICS A: PURE AND APPLIED OPTICS

J. Opt. A: Pure Appl. Opt. **4** (2002) 606–614 PII: S1464-4258(02)35611-3

Invariance analysis of improved Zernike moments

Ye Bin[1] **and Peng Jia-Xiong**

State Key Lab. for Image Processing and Intelligent Control, Institute for Pattern Recognition and Artificial Intelligence, Huazhong University of Science and Technology, Wuhan, Hubei, 430074, People's Republic of China

E-mail: Binyee@sina.com

Received 4 April 2002, in final form 30 July 2002
Published 20 September 2002
Online at stacks.iop.org/JOptA/4/606

Abstract
Zernike moments have many desirable properties, such as rotation invariance, robustness to noise, expression efficiency, fast computation and multi-level representation for describing the shapes of patterns, but there is a major drawback with Zernike moments: they need to normalize an image to achieve scale invariance. This introduces some errors since it involves the re-sampling and re-quantifying of digital images, and leads to inaccuracy of classifier. In this paper, we present improved Zernike moments, with theory and experiments that show that the improved Zernike moments not only have better rotation invariance, but also have scale invariance. Invariance of the improved Zernike moments shows great improvement over previous methods.

Keywords: Zernike moments, geometric moments, scale invariance, rotation invariance, translation invariance, trademark image

(Some figures in this article are in colour only in the electronic version)

1. Introduction

Zernike moments have a number of desirable properties: rotation invariance, robustness to noise, expression efficiency, fast computation and multi-level representation for describing various shapes of patterns [1, 3–5]. But Zernike moments have not been effectively used in image processing applications because of the drawback that they do not have scale invariance. At present, scale invariance can be achieved by scaling the original image such that its zeroth-order geometric moment is set equal to a predetermined value [2–5, 10, 11]. Zernike moments using this approach cannot well reflect the original shape in a digital image, because this approach is more suitable for an image in continuous space. For a digital image, scaling a shape introduces some errors since it involves the re-sampling and re-quantifying of the digital image, and leads to inaccuracy of classifier. For example, when a circle shape in a digital image is shrunk to some degree, it may become a square shape.

In this contribution, an improved approach is introduced to reduce the errors of rotation invariance of Zernike moments resulting from the re-sampling and re-quantifying of digital images, and to give improved Zernike moments with scale invariance. It is suitable to be applied in image retrieval systems since the improved Zernike moments then possess the desirable properties of rotation invariance, scale invariance, robustness to noise, expression efficiency, fast computation and multi-level representation for describing the various shapes of patterns.

The paper is organized as follows. Section 2 gives a definition of Zernike moments and introduces the improved Zernike moments. In section 3, the detailed theoretical proof for the invariance of the improved Zernike moments is given. Experimental details are reported in section 4, and conclusions are drawn in section 5.

2. Improvement of Zernike moments

2.1. Definition of Zernike moments

The kernel of Zernike moments is the set of orthogonal Zernike polynomials defined over the polar coordinates inside

[1] http://ia.hust.edu.cn.

a unit circle. The Zernike basis function of order p repetition q is [1]

$$V_{pq}(\rho, \theta) = R_{pq}(\rho) \exp(\mathrm{i}q\theta) \tag{1}$$

where p is a positive integer or zero, and q is an integer subject to the following constraints: $p - |q|$ is even and $|q| \leqslant p$.

R_{pq} is the radial polynomial given by

$$R_{pq}(\rho) = \sum_{s=0}^{(p-|q|)/2} \frac{(-1)^s (p-s)!}{s!(\frac{p+|q|}{2} - s)!(\frac{p-|q|}{2} - s)!} \rho^{p-2s}. \tag{2}$$

Let f be a complex-valued function on the unit disc. The Zernike moment for f of order p repetition q is

$$Z_{pq}^{(f)} = \frac{p+1}{\pi} \iint_{D^2} f(x, y) V_{pq}^*(x, y)\, \mathrm{d}x\, \mathrm{d}y \tag{3}$$

where V_{pq}^* is a complex conjugate of V_{pq}, $D^2 : x^2 + y^2 \leqslant 1$.

If F is the digital image of f, the above equation becomes

$$Z_{pq}^{(F)} = \frac{p+1}{\pi} \sum_x \sum_y F(x, y)[V_{pq}(x, y)]^* \tag{4}$$

where $x^2 + y^2 \leqslant 1$.

To calculate the Zernike moments of an image $f(x, y)$, the image (or region of interest) is first mapped to the unit disc using polar coordinates, where the centre of the image is the origin of the unit disc. Those pixels falling outside the unit disc are not used in the calculation. The magnitude of a Zernike moment is rotation invariant as reflected in the mapping of the image to the unit disc. Translation invariance is achieved by moving the origin to the centre of the image by using the centralized moments. Scale invariance can be achieved by normalizing the image.

Figure 1 shows the present approach of extracting Zernike moments from an image [11]. First, the input image is binarized. Since the Zernike moments are defined over a unit disc, the radius of a circle is determined so as to enclose the shape completely from the centroid of the binarized shape in the image to the outermost pixel of the shape. The shape is then re-sampled to normalize it to the predetermined size. The Zernike moments are then extracted from the normalized image, and the magnitudes are used as the features of pattern recognition.

Since normalization of digital images generates errors of re-sampling and re-quantifying, we can first extract Zernike moments, then normalize the moments, which will effectively eliminate the error of re-sampling and re-quantifying of digital images.

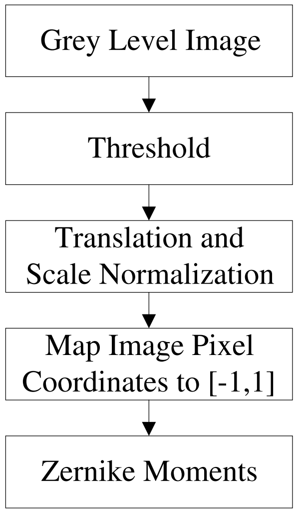

Figure 1. Block diagram of extraction of Zernike moments.

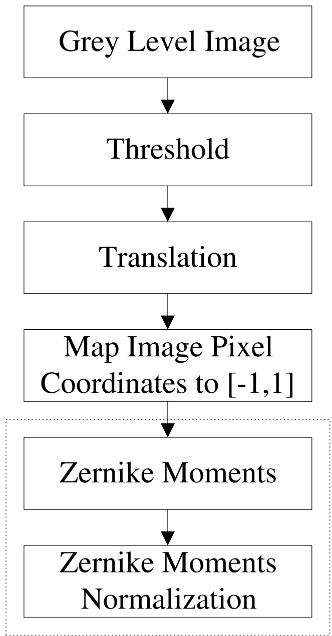

Figure 2. Block diagram of extraction of improved Zernike moments.

2.2. Improvement of Zernike moments

(1) Segment the input image to get binary image f.
(2) Move the origin of the unit disc to the centre of the shape.
(3) Calculate the zeroth-order geometric moment $g_{00}^{(f)}$ of the image f:

$$g_{00}^{(f)} = \iint_{R^2} f(x, y)\, \mathrm{d}x\, \mathrm{d}y. \tag{5}$$

(4) Calculate the various-order Zernike moments:

$$Z_{pq}^{(f)} = \frac{p+1}{\pi} \iint_{D^2} f(x, y) V_{pq}^*(x, y)\, \mathrm{d}x\, \mathrm{d}y \tag{6}$$

where $D^2 : x^2 + y^2 \leqslant 1$.

(5) Normalize the Zernike moments using $g_{00}^{(f)}$

$$Z_{pq}^{\prime(f)} = \frac{Z_{pq}^{(f)}}{g_{00}^{(f)}} \tag{7}$$

where $Z_{pq}^{\prime(f)}$ are the improved Zernike moments we have derived.

(6) Because $Z_{pq}^{\prime(f)}$ is complex, we also use the magnitudes of improved Zernike moments $|Z_{pq}^{\prime(f)}|$ as the features of shape in the pattern recognition.

Figure 2 shows the approach for extracting improved Zernike moments from an image. Lying within the dashed rectangle is the improved Zernike moments extraction.

3. Proof of invariance

3.1. Definition of geometric moments

Definition 1. *The (p+q)th geometric moment of f about* $(\bar{x}, \bar{y})$ *is given by*

$$g_{pq}^{(f)} = \iint_{R^2} (x - \bar{x})^p (y - \bar{y})^q f(x, y)\,\mathrm{d}x\,\mathrm{d}y. \tag{8}$$

The zeroth-order geometric moment is

$$g_{00}^{(f)} = \iint_{R^2} f(x, y)\,\mathrm{d}x\,\mathrm{d}y. \tag{9}$$

If we regard $f(x, y)$ *as the density at* (x, y)*, then* $g_{00}^{(f)}$ *can be thought of as the mass of the image* f*. It is thus reasonable to suppose that we can use* $g_{00}^{(f)}$ *to normalize Zernike moments.*

The first-order moments $g_{10}^{(f)}$ *and* $g_{01}^{(f)}$ *are*

$$g_{10}^{(f)} = \iint_{R^2} (y - \bar{y})^q f(x, y)\,\mathrm{d}x\,\mathrm{d}y \tag{10}$$

$$g_{01}^{(f)} = \iint_{R^2} (x - \bar{x})^p f(x, y)\,\mathrm{d}x\,\mathrm{d}y. \tag{11}$$

We can use this to abstract the idea of 'centre of mass' to images, by regarding intensity $f(x, y)$ *as density.*

Definition 2. *Calculate* $g_{00}^{(f)}$, $g_{10}^{(f)}$ *and* $g_{01}^{(f)}$ *about* $(0, 0)$*. Put*

$$x_c = \frac{g_{10}^{(f)}}{g_{00}^{(f)}} \tag{12}$$

$$y_c = \frac{g_{01}^{(f)}}{g_{00}^{(f)}}. \tag{13}$$

Then (x_c, y_c) *defines the centroid of* f*.*

3.2. Definition of radial–polar coordinate system

Definition 3. *Let f be an image. The spread of f from a point* $(\bar{x}, \bar{y})$ *is*

$$\sigma_{(\bar{x},\bar{y})}^{(f)} = \sup\left\{\rho : \rho = \sqrt{(x - \bar{x})^2 + (y - \bar{y})^2} \quad \text{where } f(x, y) > 0\right\} \tag{14}$$

where an image f *is regarded as a function from* R^2 *to* $[0, 1]$ *which has bounded support, and the spread of* f *is certainly well defined.*

Definition 4. *Let* f *be an image and* (x_c, y_c) *be its centroid. To calculate improved Zernike moments* $Z_{pq}^{\prime(f)}$*, use*

$$\rho = \frac{\sqrt{(x - x_c)^2 + (y - y_c)^2}}{\sigma_{(x_c,y_c)}^{(f)}} \tag{15}$$

$$\theta = \mathrm{atan}((y - y_c)/(x - x_c)) \tag{16}$$

as the radial–polar coordinate system.

3.3. Translation invariance

In the following section, f is an image, and f' the result of translating f by (a, b).

Lemma 1. $(x'_c, y'_c) = (x_c + a, y_c + b)$.

Proof. We note that the transformation has Jacobian 1. Calculating moments about (0, 0) in both f and f', we have

$$\begin{aligned} g_{00}^{(f')} &= \iint_{R^2} f'(x', y')\,\mathrm{d}x'\,\mathrm{d}y' \\ &= \iint_{R^2} f(x, y) 1\,\mathrm{d}x\,\mathrm{d}y = g_{00}^{(f)} \end{aligned} \tag{17}$$

and

$$\begin{aligned} g_{10}^{(f')} &= \iint_{R^2} x' f'(x', y')\,\mathrm{d}x'\,\mathrm{d}y' \\ &= \iint_{R^2} (x + a) f(x, y) 1\,\mathrm{d}x\,\mathrm{d}y \\ &= \iint_{R^2} x f(x, y)\,\mathrm{d}x\,\mathrm{d}y + a \iint_{R^2} f(x, y)\,\mathrm{d}x\,\mathrm{d}y \\ &= g_{10}^{(f)} + a g_{00}^{(f)} \end{aligned} \tag{18}$$

so

$$\frac{g_{10}^{(f')}}{g_{00}^{(f')}} = \frac{g_{10}^{(f')}}{g_{00}^{(f)}} = \frac{g_{10}^{(f)}}{g_{00}^{(f)}} + a \tag{19}$$

and hence

$$x'_c = x_c + a. \tag{20}$$

Similarly

$$y'_c = y_c + b. \tag{21}$$

□

Proposition 2. *Calculate* $g_{pq}^{(f')}$ *about the centroid* (x'_c, y'_c) *of* f'*, and* $g_{pq}^{(f)}$ *about the centroid* (x_c, y_c) *of* f*. Then* $g_{pq}^{(f')} = g_{pq}^{(f)}$*.*

Proof.

$$\begin{aligned} &g_{pq}^{(f')} \text{ about } (x'_c, y'_c) \\ &= \iint_{R^2} (x' - x'_c)^p (y' - y'_c)^q f'(x', y')\,\mathrm{d}x'\,\mathrm{d}y' \end{aligned} \tag{22}$$

and applying lemma 1,

$$\begin{aligned} &g_{pq}^{(f')} \text{ about } (x'_c, y'_c) \\ &= \iint_{R^2} ((x + a) - (x_c + a))^p ((y + b) \\ &\quad - (y_c + b))^q f(x, y)\,\mathrm{d}x\,\mathrm{d}y \\ &= \iint_{R^2} (x - x_c)^p (y - y_c)^q f(x, y)\,\mathrm{d}x\,\mathrm{d}y \\ &= g_{pq}^{(f)} \text{ about } (x_c, y_c). \end{aligned} \tag{23}$$

From the above formula, we can see that the central geometric moments possess translation invariance. The translation invariance of improved Zernike moments can be achieved by moving the origin to the centre of the image by using the centralized moments. □

3.4. Scale invariance

In the following section, f is an image, and f' the result of scaling f by α.

Proposition 3. *Let $(\bar{x}, \bar{y}) \in R^2$, mapping to $(\bar{x}', \bar{y}')$ under scaling. Calculate $g_{pq}^{(f)}$ about $(\bar{x}, \bar{y})$ and $g_{pq}^{(f')}$ about $(\bar{x}', \bar{y}')$, then $g_{pq}^{(f')} = \alpha^{p+q+2} g_{pq}^{(f)}$.*

Proof. From f' is the result of scaling f by α, we can get

$$\begin{aligned} x' &= \alpha x \\ y' &= \alpha y. \end{aligned} \tag{24}$$

We note that the transformation has Jacobian α^2. So

$$\begin{aligned} g_{pq}^{(f')} &= \iint_{R^2} (x' - \bar{x}')(y' - \bar{y}') f(x', y')\,\mathrm{d}x'\,\mathrm{d}y' \\ &= \iint_{R^2} (\alpha x - \alpha\bar{x})^p (\alpha y - \alpha\bar{y})^q f(x, y) \alpha^2\,\mathrm{d}x\,\mathrm{d}y \\ &= \alpha^{p+q+2} g_{pq}^{(f)}. \end{aligned} \tag{25}$$

□

Corollary 4. *The scale factor from f to f' is*

$$\alpha = \sqrt{\frac{g_{00}^{(f')}}{g_{00}^{(f)}}}. \tag{26}$$

Proof. The proof follows immediately from $g_{00}^{(f')} = \alpha^2 g_{00}^{(f)}$. □

Lemma 5. *$(x_c', y_c') = (\alpha x_c, \alpha y_c)$.*

Proof. We note that (0, 0) for f maps to (0, 0) for f' under scaling. So, calculating about (0, 0) for each of f and f' using proposition 2, we have

$$g_{00}^{(f')} = \alpha^2 g_{00}^{(f)} \tag{27}$$

$$g_{10}^{(f')} = \alpha^{1+2} g_{10}^{(f)}$$

$$\frac{}{g_{00}^{(f')}} = \frac{\alpha^{1+2} g_{10}^{(f)}}{\alpha^2 g_{00}^{(f)}} = \alpha x_c \tag{30}$$

$$y_c' = \frac{g_{01}^{(f')}}{g_{00}^{(f')}} = \frac{\alpha^{1+2} g_{01}^{(f)}}{\alpha^2 g_{00}^{(f)}} = \alpha y_c. \tag{31}$$

□

Lemma 6.
$\sqrt{(x' - x_c')^2 + (y' - y_c')^2} = \alpha\sqrt{(x - x_c)^2 + (y - y_c)^2}$.

Proof. Using lemma 5,

$$\begin{aligned} (x' - x_c')^2 + (y' - y_c')^2 &= (\alpha x - \alpha x_c)^2 + (\alpha y - \alpha y_c)^2 \\ &= \alpha^2((x - x_c)^2 + (y - y_c)^2) \end{aligned} \tag{32}$$

and the required result follows from taking square roots on both sides. □

Lemma 7. $\sigma_{(x_c', y_c')}^{(f')} = \alpha\sigma_{(x_c, y_c)}^{(f)}$.

Proof. Using lemma 6 and noting that $f'(x', y') = f(x, y)$, we have

$$\begin{aligned} \sigma_{(x_c', y_c')}^{(f')} &= \sup\left\{\rho' : \rho' = \sqrt{(x' - x_c')^2 + (y' - y_c')^2} \right. \\ &\qquad \left. \text{where } f'(x', y') > 0\right\} \\ &= \sup\left\{\alpha\rho : \rho = \sqrt{(x - x_c)^2 + (y - y_c)^2} \right. \\ &\qquad \left. \text{where } f(x, y) > 0\right\} = \alpha\sigma_{(x_c, y_c)}^{(f)}. \end{aligned}$$

$$\begin{aligned} &\frac{\overline{(x' - x_c')^2 + (y' - y_c')^2}}{\sigma_{(x_c' - x_c)}^{(f')}} \\ &= \frac{\alpha\sqrt{(x - x_c)^2 + (y - y_c)^2}}{\alpha\sigma_{(x_c - x_c)}^{(f)}} = \rho. \end{aligned} \tag{34}$$

By lemma 5,

$$\begin{aligned} \theta' &= a\tan((y' - y_c')/(x' - x_c')) \\ &= a\tan((\alpha y - \alpha y_c)/(\alpha x - \alpha x_c)) \\ &= a\tan((y - y_c)/(x - x_c)) = \theta. \end{aligned} \tag{35}$$

□

Proposition 9. $Z_{pq}^{(f')} = \alpha^2 Z_{pq}^{(f)}$.

Proof. By lemma 8, $\rho' = \rho$ and $\theta' = \theta$, so

$$R_{pq}(\rho') = R_{pq}(\rho) \tag{36}$$

$$\exp(\mathrm{i}q\theta') = \exp(\mathrm{i}q\theta) \tag{37}$$

and hence

$$V_{pq}(\rho', \theta') = V_{pq}(\rho, \theta). \tag{38}$$

By definition, $f'(x', y') = f(x, y)$, and we note that the Jacobian of the transformation is α^2. So

$$\begin{aligned} Z_{pq}^{(f')} &= \frac{p+1}{\pi} \iint_{\rho' \leqslant 1} f'(x', y') V_{pq}^*(\rho', \theta')\,\mathrm{d}x'\,\mathrm{d}y' \\ &= \frac{p+1}{\pi} \iint_{\rho' \leqslant 1} f(x, y) V_{pq}^*(\rho, \theta) \alpha^2\,\mathrm{d}x\,\mathrm{d}y = \alpha^2 Z_{pq}^{(f)}. \end{aligned} \tag{39}$$

□

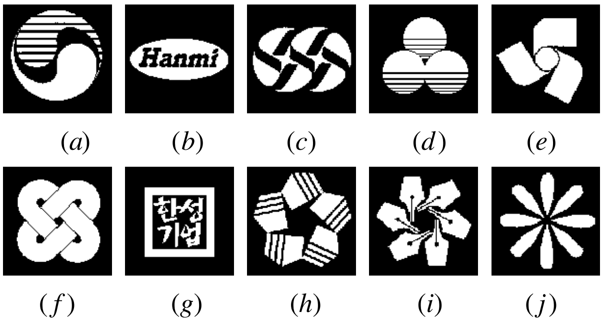

Figure 3. First 10 trademark images of the test.

Proposition 10. $Z'^{(f')}_{pq} = Z'^{(f)}_{pq}$.

Proof. By proposition 9 and corollary 4, we have

$$Z'^{(f')}_{pq} = \frac{Z^{(f')}_{pq}}{g^{(f')}_{00}} = \frac{\alpha^2 Z^{(f)}_{pq}}{g^{(f')}_{00}} = \frac{\frac{g^{(f')}_{00}}{g^{(f)}_{00}} Z^{(f)}_{pq}}{g^{(f')}_{00}} = \frac{Z^{(f)}_{pq}}{g^{(f)}_{00}} = Z'^{(f)}_{pq}. \quad (40)$$

Note that the relationship between scaled improved Zernike moments is independent of p and q. This is in contrast to geometric moments, as we saw in proposition 3.

From the above formula we can find that improved Zernike moments possess scale invariance. □

Proposition 11. $Z'^{(f)}_{00} = \frac{1}{\pi}$, $Z'^{(f)}_{11} = Z'^{(f)}_{1-1} = 0$.

Proof. Let $p = q = 0$ and $p = 1, q = \pm 1$, calculate formulae (7)–(9), and we get the result. □

3.5. Rotation invariance

In the following developments, f is an image and f' the result of rotating f by φ about $(\bar{x}, \bar{y})$.

Lemma 12. $\begin{pmatrix} x'_c \\ y'_c \end{pmatrix} = R^{(\bar{x},\bar{y})}_{\varphi} \begin{pmatrix} x_c \\ y_c \end{pmatrix}$.

Proof. We note that the transformation has Jacobian

$$\begin{vmatrix} \cos\varphi & -\sin\varphi \\ \sin\varphi & \cos\varphi \end{vmatrix} = 1 \quad (41)$$

and we have

$$\begin{aligned} x' &= \cos\varphi(x - \bar{x}) - \sin\varphi(y - \bar{y}) + \bar{x} \\ y' &= \sin\varphi(x - \bar{x}) + \cos\varphi(y - \bar{y}) + \bar{y}. \end{aligned} \quad (42)$$

Calculating moments about (0, 0) in both f and f', we have

$$\begin{aligned} g^{(f')}_{00} &= \iint_{R^2} f'(x', y')\, dx'\, dy' \\ &= \iint_{R^2} f(x, y)\, dx\, dy = g^{(f)}_{00} \end{aligned} \quad (43)$$

and

$$\begin{aligned} g^{(f')}_{10} &= \iint_{R^2} x' f'(x', y')\, dx'\, dy' \\ &= \iint_{R^2} (\cos\varphi(x - \bar{x}) \\ &\quad - \sin\varphi(y - \bar{y}) + \bar{x}) f(x, y) \cdot 1 \cdot dx\, dy \\ &= \cos\varphi \iint_{R^2} x f(x, y)\, dx\, dy - \cos\varphi\bar{x} \\ &\quad \times \iint_{R^2} f(x, y)\, dx\, dy - \sin\varphi \iint_{R^2} y f(x, y)\, dx\, dy \\ &\quad + \sin\varphi\bar{y} \iint_{R^2} f(x, y)\, dx\, dy + \bar{x} \iint_{R^2} f(x, y)\, dx\, dy \\ &= \cos\varphi(g^{(f)}_{10} - \bar{x} g^{(f)}_{00}) - \sin\varphi(g^{(f)}_{01} - \bar{y} g^{(f)}_{00}) + \bar{x} g^{(f)}_{00} \end{aligned} \quad (44)$$

so

$$\frac{g^{(f')}_{10}}{g^{(f')}_{00}} = \frac{g^{(f')}_{10}}{g^{(f)}_{00}} = \cos\varphi\left(\frac{g^{(f)}_{00}}{g^{(f)}_{10}} - \bar{x}\right) - \sin\varphi\left(\frac{g^{(f)}_{00}}{g^{(f)}_{01}} - \bar{y}\right) + \bar{x} \quad (45)$$

and hence

$$x'_c = \cos\varphi(x_c - \bar{x}) - \sin\varphi(y_c - \bar{y}) + \bar{x}. \quad (46)$$

Similarly

$$y'_c = \sin\varphi(x_c - \bar{x}) + \cos\varphi(y_c - \bar{y}) + \bar{y}. \quad (47)$$

□

Lemma 13. $\sqrt{(x' - x'_c)^2 + (y' - y'_c)^2} = \sqrt{(x - x_c)^2 + (y - y_c)^2}$.

Proof. By lemma 12,

$$\begin{aligned} &(x' - x'_c)^2 + (y' - y'_c)^2 \\ &= (\cos\varphi(x - \bar{x}) - \sin\varphi(y - \bar{y}) + \bar{x} \\ &\quad - \cos\varphi(x_c - \bar{x}) + \sin\varphi(y_c - \bar{y}) - \bar{x})^2 \\ &\quad + (\sin\varphi(x - \bar{x}) + \cos\varphi(y - \bar{y}) + \bar{y} \\ &\quad - \sin\varphi(x_c - \bar{x}) + \cos\varphi(y_c - \bar{y}) - \bar{y})^2 \\ &= (\cos\varphi(x - x_c) - \sin\varphi(y - y_c))^2 \\ &\quad + (\sin\varphi(x - x_c) + \cos\varphi(y - y_c))^2 \\ &= \cos^2\varphi(x - x_c)^2 - 2\cos\varphi\sin\varphi(x - x_c)(y - y_c) \\ &\quad + \sin^2\varphi(y - y_c)^2 + \sin^2\varphi(x - x_c)^2 \\ &\quad + 2\sin\varphi\cos\varphi(x - x_c)(y - y_c) + \cos^2\varphi(y - y_c)^2 \\ &= (x - x_c)^2 + (y - y_c)^2 \end{aligned} \quad (48)$$

and the required result follows from taking square roots on both sides. □

Lemma 14. $\sigma^{(f')}_{(x'_c, y'_c)} = \sigma^{(f)}_{(x_c, y_c)}$.

Proof. Using lemma 13 and noting that $f'(x', y') = f(x, y)$, we have

$$\begin{aligned} \sigma^{(f')}_{(x'_c, y'_c)} &= \sup\left\{\rho' : \rho' = \sqrt{(x' - x'_c)^2 + (y' - y'_c)^2}\right. \\ &\quad \left.\text{where } f'(x', y') > 0\right\} \\ &= \sup\left\{\rho' : \rho = \sqrt{(x - x_c)^2 + (y - y_c)^2}\right. \\ &\quad \left.\text{where } f(x, y) > 0\right\} = \sigma^{(f)}_{(x_c, y_c)}. \end{aligned} \quad (49)$$

□

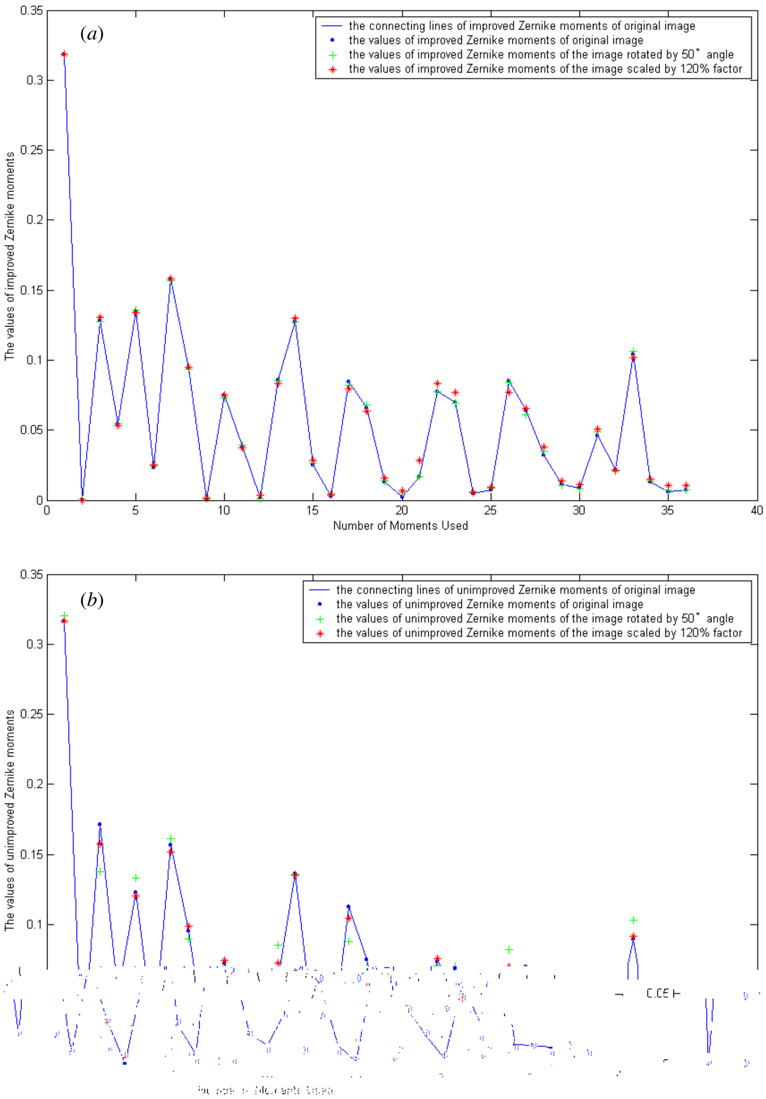

Figure 4. Invariance of Zernike moments of the trademark shown in figure 3(*a*). (*a*) Improved Zernike moments; (*b*) unimproved Zernike moments.

Lemma 15. *$\rho' = \rho$ and $\theta' = \theta + \varphi$, when using definition 4.*

Proof. By lemmas 13 and 14, we have

$$\rho' = \frac{\sqrt{(x' - x_c')^2 + (y' - y_c')^2}}{\sigma^{(f')}_{(x_c', y_c')}} = \frac{\sqrt{(x - x_c)^2 + (y - y_c)^2}}{\sigma^{(f)}_{(x_c, y_c)}} = \rho. \tag{50}$$

By lemma 12

$$\begin{aligned} y' - y_c' &= \sin\varphi(x - \bar{x}) + \cos\varphi(y - \bar{y}) + \bar{y} \\ &\quad - \sin\varphi(x_c - \bar{x}) - \cos\varphi(y_c - \bar{y}) - \bar{y} \\ &= \sin\varphi(x - x_c) + \cos\varphi(y - y_c) \end{aligned} \tag{51}$$

and

$$\begin{aligned} x' - x_c' &= \cos\varphi(x - \bar{x}) + \sin\varphi(y - \bar{y}) + \bar{x} \\ &\quad - \cos\varphi(x_c - \bar{x}) + \sin\varphi(y_c - \bar{y}) - \bar{x} \\ &= \cos\varphi(x - x_c) - \sin\varphi(y - y_c) \end{aligned} \tag{52}$$

so

$$\begin{aligned} \theta' &= a\tan((y' - y_c')/(x' - x_c')) \\ &= a\tan((\sin\varphi(x - x_c) + \cos\varphi(y - y_c)) \\ &\quad \times (\cos\varphi(x - x_c) - \sin\varphi(y - y_c))^{-1}) \\ &= a\tan\left(\left(\frac{\sin\varphi}{\cos\varphi}\frac{x - x_c}{x - x_c} + \frac{\cos\varphi}{\cos\varphi}\frac{y - y_c}{x - x_c}\right)\right. \\ &\quad \left. \times \left(\frac{\cos\varphi}{\cos\varphi}\frac{x - x_c}{x - x_c} - \frac{\sin\varphi}{\cos\varphi}\frac{y - y_c}{x - x_c}\right)^{-1}\right) \\ &= a\tan((\tan\varphi + \tan\theta)/(1 - \tan\varphi\tan\theta)) \\ &= a\tan(\tan(\theta + \varphi)) = \theta + \varphi. \end{aligned} \tag{53}$$

□

Proposition 16. $Z^{(f')}_{pq} = Z^{(f)}_{pq}\exp(-\mathrm{i}q\varphi)$.

Proof. By lemma 15, $\rho' = \rho$ and $\theta' = \theta + \varphi$, so

$$R_{pq}(\rho') = R_{pq}(\rho) \tag{54}$$

$$\exp(\mathrm{i}q\theta') = \exp(\mathrm{i}q(\theta + \varphi)) = \exp(\mathrm{i}q\theta)\exp(\mathrm{i}q\varphi) \tag{55}$$

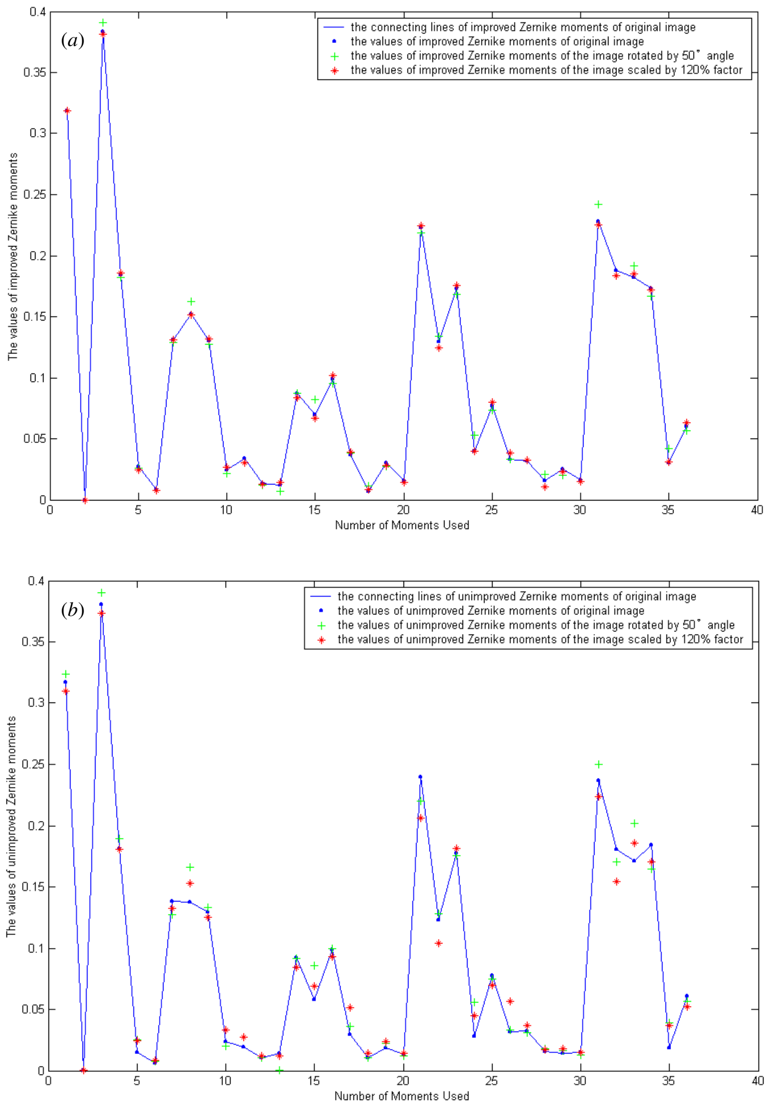

Figure 5. Invariance of Zernike moments of the trademark shown in figure 3(*b*). (*a*) Improved Zernike moments; (*b*) unimproved Zernike moments.

and hence

$$V_{pq}(\rho', \theta') = V_{pq}(\rho, \theta)\exp(\mathrm{i}q\varphi). \tag{56}$$

By definition, $f'(x', y') = f(x, y)$, and we note that the Jacobian of the transformation is 1. So

$$\begin{aligned} Z_{pq}^{(f')} &= \frac{p+1}{\pi}\iint_{\rho'\leqslant 1} f'(x', y')V_{pq}^{*}(\rho', \theta')\,\mathrm{d}x'\,\mathrm{d}y' \\ &= \frac{p+1}{\pi}\iint_{\rho'\leqslant 1} f(x, y)V_{pq}^{*}(\rho, \theta)\exp(-\mathrm{i}q\varphi)\cdot 1\cdot \mathrm{d}x'\,\mathrm{d}y' \\ &= Z_{pq}^{(f)}\exp(-\mathrm{i}q\varphi). \end{aligned} \tag{57}$$

□

Proposition 17. $Z_{pq}'^{(f')} = Z_{pq}'^{(f)}\exp(-\mathrm{i}q\varphi)$.

Proof. By proposition 16 and corollary 4, we have

$$Z_{pq}'^{(f')} = \frac{Z_{pq}^{(f')}}{g_{00}^{(f')}} = \frac{Z_{pq}^{(f)}\exp(-\mathrm{i}q\varphi)}{g_{00}^{(f)}} = Z_{pq}'^{(f)}\exp(-\mathrm{i}q\varphi). \tag{58}$$

□

Corollary 18. $|Z_{pq}'^{(f')}| = |Z_{pq}'^{(f)}|$.

Proof. The proof follows immediately from $|\exp(-\mathrm{i}q\varphi)| = 1$. □

From corollary 18 we can find that the magnitudes of improved Zernike moments possess rotation invariance.

4. Experimental details

To evaluate the performance of the proposed improved Zernike moments, experiments were conducted. The test image database consists of about 3000 trademark-type images (that contain graphical or figurative elements only) in MPEG-7 test material ITEM S8 [9]. The first 10 trademark images are shown in figure 3.

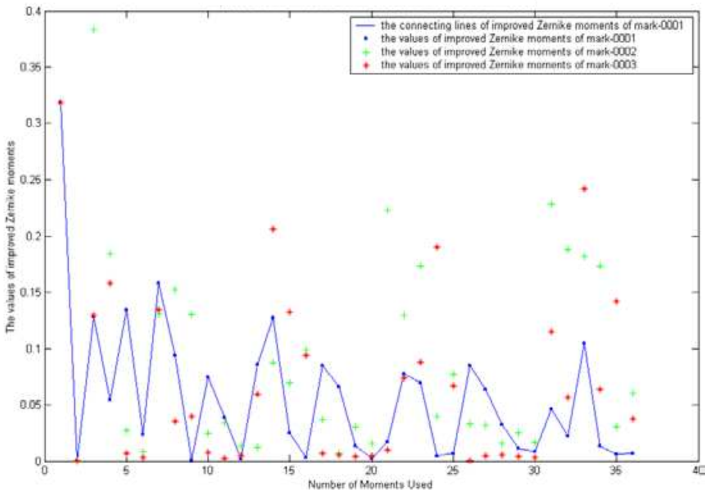

Figure 6. Different values of improved Zernike moments of the trademarks shown in: • figure 3(a); + figure 3(b); ∗ figure 3(c).

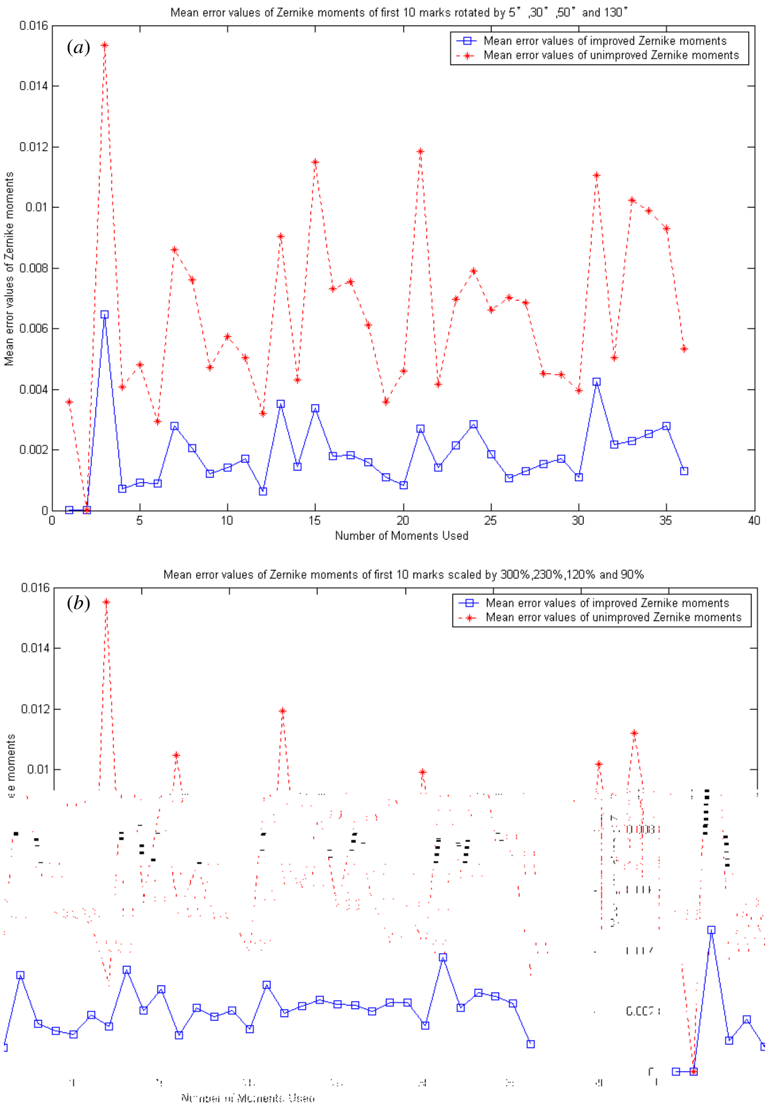

Figure 7. Mean error values of improved and unimproved Zernike moments. (a) Mean error values of the first 10 trademark images rotated. (b) Mean error values of the first 10 trademark images scaled.

The experiments were as follows:

Step 1. Image transformations:

(1) Rotation—the image is rotated by 5°, 30°, 50° and 130°.
(2) Scale—the image is scaled by 500, 230, 120 and 90%.
(3) Rotation/scale—the image is first rotated by 60°, then scaled by 500%.

Step 2. Computation of improved and unimproved Zernike moments of the transformed images: 36 moments (order $p = 0 \ldots 10$) are computed.

Step 3. Analysis of improved and unimproved Zernike moments: plot the values of them to show the invariance properties.

Figures 4 and 5 show the values of the improved and unimproved Zernike moments of figures 3(*a*) and (*b*) respectively. Here we only show the values of moments of the original image, the image rotated by 50° and the image scaled by 120%. From figures 4(*a*) and 5(*a*), we can see that the differences of the improved corresponding Zernike moments of the transformed images are very small, and it is difficult to show all of the discrepancy. In particular, the values of the image scaled by 120% are almost the same as those of the original image, which indicates that the improved Zernike moments possess very good scale invariance. Figures 4(*b*) and 5(*b*) show the values of unimproved Zernike moments of figures 3(*a*) and (*b*) respectively. Comparing these with figures 4(*a*) and 5(*a*), we can see that the improved Zernike moments possess better rotation invariance and scale invariance properties than the unimproved Zernike moments.

Figure 6 shows the values of the different improved Zernike moments of figures 3(*a*)–(*c*). From this figure we can see that the improved Zernike moments of these trademark images are obviously different. Except for $Z'^{(f)}_{00} = 0.318$ and $Z'^{(f)}_{11} = 0$, they can be selected as good feature descriptors of pattern recognition.

Figure 7 shows the mean error values of improved and unimproved Zernike moments for the first 10 trademark images rotated and scaled respectively. From this figure we can see the mean error values of the improved Zernike moments are smaller than those of the unimproved moments.

5. Conclusion

In this paper, we have discussed the drawbacks of the existing approach to extracting Zernike moments, and proposed an approach for improved Zernike moments. A detailed theoretical proof about the invariance of improved Zernike moments is given. The performance of the improved Zernike moments is experimentally examined using trademark images, and it is shown that the invariance of the improved Zernike moments has been greatly improved over present methods.

References

[1] Mukundan R and Ramakrishnan K R 1998 *Moment Functions in Image Analysis—Theory and Applications* (Singapore: World Scientific)

[2] Abu-Mostafa Y S and Psaltis D 1985 Image normalization by complex moments *IEEE Trans. Pattern Anal. Mach. Intell.* **7** 46–55

[3] Teh C H and Chin R T 1988 On image analysis by the method of moments *IEEE Trans. Pattern Anal. Mach. Intell.* **10** 496–513

[4] Belkasim S O 1991 Pattern recognition with moment invariants—a comparative study and new results *Pattern Recognit.* **24** 1117–38

[5] Khotanzad A 1990 Invariant image recognition by Zernike moments *IEEE Trans. Pattern Anal. Mach. Intell.* **12** 489–97

[6] Khotanzad A and Hong Y H 1990 Rotation invariant image recognition using features selected via a systematic method *Pattern Recognit.* **23** 1089–101

[7] Leu J G 1991 Computing a shape's moments from its boundary *Pattern Recognit.* **24** 949–57

[8] Prata A and Rusch W V T 1989 Algorithm for computation of Zernike polynomials expansion coefficients *Appl. Opt.* **28** 749–54

[9] Jeannin S 1999 MPEG-7 visual part of experimental model version 2.0, ISO/IEC JTC1/SC29/WG11/N2822 (*Vancouver*)

[10] Kim Yong-Sung and Kim Whoi-Yul 1998 Content-based trade-mark retrieval system using visually salient feature *J. Image Vis. Comput.* **16** 12–13

[11] Kim Whoi-Yul and Kim Yong-Sung 2000 A region-based shape descriptor using Zernike moments *Signal Process., Image Commun.* **16** 95–102

[12] Bailey R R and Srinath M 1996 Orthogonal moment features for use with parametric and non-parametric classifiers *IEEE Trans. Pattern Anal. Mach. Intell.* **18** 389–99

[13] Cash G L and Hatamian M 1987 Optical character recognition by the method of moments *Comput. Vis. Graph. Image Process.* **59** 291–310

[14] Khotanzad A and Lu J 1990 Classification of invariant image representations using a neural network *IEEE Trans. on Acoust. Speech Signal Process.* **38** 1028–38

[15] Mukundan R and Ramakrishnan K R 1995 Fast computation of Legendre and Zernike moments *Pattern Recognit.* **28** 1433–42